# Modeling of the solitary waves trajectories in “shallow water” environments

https://doi.org/10.31713/MCIT.2023.027

Yurii Turbal
Computer Science and Applied Mathematic departament
National University of Water and Environmental Engineering
Rivne, Ukraine
turbaly@gmail.com

Mariana Turbal
Computer Science and Applied Mathematic departament
National University of Water and Environmental Engineering
Rivne, Ukraine
Turbal.mariana.1@gmail.com

Andrii Bomba
Computer Science and Applied Mathematic departament
National University of Water and Environmental Engineering
Rivne, Ukraine
abomba@ukr.net

*Abstract*—**Solitary waves in the “shallow water” environment are considered and approximate approach to calculation and prediction of trajectories of these waves is proposed. We use an approach which was developed in recent years and was called the T-representations method. This method allows to move away from the exact solutions of the corresponding systems of differential equations and construct the trajectory approximately, in fact estimating only the point of maximum of the wave amplitude and its displacement. An appropriate mathematical simplification makes efficient computer simulations possible. In recent years, software packages have been actively used to monitor and predict a number of dangerous natural phenomena, such as Earth Alerts, Pacific Tsunami Warning System, Wave Monitoring Sites and others. But these systems do not take solitary waves into account. Using our approach, it is possible to refine the parameters of solitary waves in a specific environment, investigate whether such waves exist there at all and create functions taking into account solitary waves in monitoring systems.**

**Keywords—solitary wave; shallow water; T-representation; trajectory prediction; software.**

## I. Introduction

Software packages containing prediction modules that use the properties of localized soliton-like waves have been actively developed [12]. In this case, localized soliton-like perturbations are considered in various aspects. In the study of seismic processes [15, 16] for example, a separate wave can be considered as a generator of seismic shock, if it passes through the zone of accumulation of seismic energy. A similar effect can occur when several waves hit an area at the same time, because then there may be cracks in the earth's crust and, accordingly, seismic shocks (such an effect occurred, for example, in an earthquake in Fukushima Prefecture, Japan in 2016). In such cases, it is important to identify the soliton and predict its trajectory. Information about the trajectories of isolated waves and the nature of their movement is of great practical importance in cases where the isolated waves themselves pose a danger (such as a tsunami) [1, 2]. If the soliton occurs on the surface of water, it can also be dangerous, for example, in the case of the so-called killer wave, studied in the MaxWave project [1]. Therefore, the study of the trajectories of localized waves is a very important task.

The problem of modeling the processes of origin and propagation of isolated waves has several aspects, in particular, an analytical description of the wave profile and the presence of a number of specific properties of soliton [3 – 7], which are guaranteed by some methods at the stage of their application and do not require further study. The presence of such methods determines their complexity. Mathematical models that describe the propagation of isolated waves are divided into two classes: integrated and non-integrated using the method of the inverse scattering problem [2 – 7, 10, 11] in collisions they retain their characteristics and there is only a phase shift. Many papers have shown that in integrated models localized waves behave like particles. This fact has been confirmed in numerous experiments in which plasma waves, liquid with gas bubbles, stratified liquid and electromagnetic waves have been studied. At the same time, for systems that do not integrate using the inverse scattering problem, a number of other effects occur, including radiation of nonlinear wave trains, splitting of individual waves and formation of new soliton-like waves, merging of several waves and formation of a new series of elastic reflections.

At the same time, the wave profile may change over time, then such a wave will no longer be a soliton in the classical sense, but may have soliton properties that require further study. Soliton solutions of equations considered in the framework of the structural-phenomenological approach, for example, are isolated partial cases of solutions and do not make it possible to solve the problem of formation of a separate wave from an arbitrary initial perturbation. The use of δ-solitons in the asymptotic case allows you to ignore the shape of the wave profile. However, general functions as models

of real physical phenomena have a number of disadvantages, including infinity, specific mathematical content of derivatives, and others.

The analytical description of isolated waves in multidimensional cases is especially problematic now [2]. Even for a well-studied system of equations such as "shallow water" [1, 14], periodic analytical solutions have only recently been found and the author does not know the methods of analytical study of isolated waves.

## II. T-FORMS FOR THE SHALLOW WATER ENVIRONMENTS

A number of approaches to finding soliton solutions of the corresponding differential equations are known today. The method of the inverse scattering problem plays a fundamental role. There is an infinite number of differential equations that can be differentiated using this method. However, the method does not exhaust all the equations that soliton solutions can have. In addition, there are other methods that allow us to find both exact and approximate soliton solutions of differential equations. However, the corresponding methods are often special in nature and are effective only for a certain class of equations. Most of them relate to the one-dimensional case.

In recent years, in order to constructively study the trajectories of localized soliton-like perturbations, a slightly different approach has been proposed, called the T-representation method. This method has approximate variants when the solutions are Gaussian and can easily be extended to multidimensional cases.

In [12], a method for finding solutions of equations of motion is presented in the form of:

$$(u^{(1)},u^{(2)},...,u^{(m)})^T = \\ = (\psi_1(t),\psi_2(t),...,\psi_m(t))^T W(x_1,x_2,...,x_n,t), \quad (1)$$

where $u^{(1)},u^{(2)},...,u^{(m)}$ are the displacements in the Cartesian coordinate system,

$$W(x_1,x_2,...,x_n,\tilde{x}_1(t),\tilde{x}_2(t),...,\tilde{x}_n(t),t) = \\ = \exp(-\mu((x_1,x_2,...,x_n),(\tilde{x}_1(t),\tilde{x}_2(t),...,\tilde{x}_n(t)))/\varepsilon),$$

$\mu(a,b)$ is a measure defined on a set of intervals $\{[a.b], a,b \in R^n\}$, ( $\mu(\alpha,\beta)=0$ if $\alpha=\beta$ ), $\psi_1(t)$, $\psi_2(t)$, …, $\psi_m(t)$ are functions that determine the components of the amplitude of the corresponding perturbations, $\varepsilon$ is a parameter that determines the localization of the perturbation, $\tilde{x}_1(t)$, $\tilde{x}_2(t)$ ,…, $\tilde{x}_n(t)$ are functions that determine the trajectory of the point of maximum perturbation.

The solution in the form (1) defines a localized wave, the maximum of which is at a point $(\tilde{x}_1(t),\tilde{x}_2(t),...,\tilde{x}_n(t))$. Note that in the case of an arbitrary measure $\mu$, in form (1) we can represent an arbitrary solution that has the character of a unimodal isolated wave, the shape of which does not change with time. The measure $\mu$ determines the form of perturbation. We can consider a more general case when the functions $\tilde{x}_i(.)$ depend not only on time but also on spatial coordinates $\tilde{x}_i(t)=\tilde{x}_i(x_1,x_2,...,x_n,t)$

Shallow water equations are of great practical importance because they describe large-scale atmospheric and ocean currents, particularly in midlatitudes. In Cartesian coordinates, they have the form [15]:

$$\begin{aligned} &u_t + uu_x + vu_y + gh_x = fv, \\ &v_t + uv_x + vv_y + gh_y = -fu, \\ &h_t + (uh)_x + (vh)_y = 0, \end{aligned} \quad (2)$$

where $u$, $v$ are components of the velocity vector, $h$ is the depth of the liquid layer above the flat bottom; f is the Coriolis parameter (rotation frequency), g is the acceleration of free fall. The approximate model (2) is obtained from Euler's equations [14] of an ideal fluid under the following assumptions: the ratio of the characteristic vertical scale of the flow to the characteristic horizontal scales is much less than 1; the density of the liquid became; the pressure in the liquid is hydrostatic at depth; the axis of rotation coincides with the vertical axis z.

Note that the shallow water equations are usually solved by numerical methods due to significant difficulties in obtaining analytical solutions. In recent years, group theory methods have been used to analyze shallow water-type equations [13 – 15]. In particular, with the help of group analysis methods the Lie algebra in the absence of rotation is constructed, in [14] a system of subalgebras containing 179 representatives is constructed. On the basis of the corresponding algebra, periodic exact solutions are constructed, which can be interpreted as pulsations of a liquid under the action of gravity or Coriolis.Numerical methods for solving shallow water equations show that there are solutions that simulate isolated waves, such as circular tsunami waves.

The system of shallow water equations can easily be generalized to the case of polytropic gas flow, which is considered in the barotropic approximation. The motion of a compressible viscous gas can be conveniently studied in the polar coordinate system.

Such problems include a number of applied engineering and geophysical problems, including the study of atmospheric phenomena on a planetary scale, the study of astrophysical objects associated with the motion of matter around the center of gravity, including the gas disks of galaxies. The shallow water type equations in the polar coordinate system will look like this:

$$\begin{aligned} &\frac{\partial\sigma}{\partial t} + \sigma\left(\frac{\partial u}{\partial r} + \frac{u}{r} + \frac{\partial v}{r\partial\varphi}\right) + u\frac{\partial\sigma}{\partial r} + \frac{v\partial\sigma}{r\partial\varphi} = 0, \\ &\frac{\partial u}{\partial t} + u\frac{\partial u}{\partial r} + \frac{v}{r}\frac{\partial u}{\partial\varphi} - \frac{v^2}{r} = -\frac{\partial\Phi}{\partial r} - B\gamma_s\sigma^{\gamma_s-2}\frac{\partial\sigma}{\partial r} \\ &\frac{\partial v}{\partial t} + u\frac{\partial v}{\partial r} + \frac{v}{r}\frac{\partial v}{\partial\varphi} + \frac{uv}{r} = -\frac{1}{r}\frac{\partial\Phi}{\partial\varphi} - \sigma^{\gamma_s-2}\frac{B\gamma_s}{r}\frac{\partial\sigma}{\partial\varphi}, \end{aligned} \quad (3)$$

where $u(r,\varphi,t)$ , $v(r,\varphi,t)$ are radial and azimuthal components of gas velocity, respectively, $\sigma(r,\varphi,t)$ is surface density of the gas disk, $\Phi(r,\varphi,t)$ is potential that describes the action of an external force, $B, D$ are positive constants. Note that system (3) is quasilinear.

Based on the above-described method of T-representations, the vector-function of perturbations will be found in the form:

$$f_1(r,\varphi,t) = \varepsilon_0 \psi_f(t)\omega(r,\varphi,t,\varepsilon), \tag{4}$$

where $\psi_f(t) = (\psi_u(t), \psi_v(t), \psi_\sigma(t))$ , $\psi_u(t)$ , $\psi_v(t)$ , $\psi_\sigma(t)$ , $\tilde{r}(t)$ , $\tilde{\varphi}(t)$ are any functions, $\tilde{r}(t) \geq 0$ , $\psi_\sigma(t) \geq 0$ , $\varepsilon$ is small parameter, $\varepsilon_0$ is constant, $\omega(r,\varphi,t,\varepsilon) = \exp\{-\frac{g(r-\tilde{r}(t)) + g(\varphi-\tilde{\varphi}(t))}{\varepsilon}\}$ , $g(x)$ is a function that has properties:

1. $g(x) \geq 0$ , $x \in (-\infty,+\infty)$ ,
2. $g(0) = 0$ ,
3. $g(-x) = g(x)$ ,
4. Exists constants $\alpha_1, \tilde{\alpha}_1$ , $\alpha_2, \tilde{\alpha}_2$ , $c_1 > 0$ , $c_2 > 0$ , $\varepsilon > 0$ those that,

$$\tilde{c}_1 g^{\tilde{\alpha}_1}(x) \leq |g'(x)| \leq c_1 g^{\alpha_1}(x), |g''(x)| \leq c_2 g^{\alpha_2}(x)$$

in region $\{x : g(x) \leq -\varepsilon \ln \varepsilon\}$ .

We see that in this case the perturbation is a single wave, and the point of maximum perturbation moves along the trajectory described in the polar coordinate system by the functions $\tilde{r}(t)$ and $\tilde{\varphi}(t)$ .

## III. Analisis of the trajectory of localized waves

As a result of substituting (4) into the system (3) and taking into account the properties of the function g(), we can obtain systems:

$$\begin{cases} \psi_\sigma'(t) + \sigma_0 \dfrac{\psi_u(t)}{r} + \psi_u(t)\dfrac{\partial \sigma_0}{\partial r} + \dfrac{\psi_v(t)}{r}\dfrac{\partial \sigma_0}{\partial \varphi} + \\ + \dfrac{1}{r}\varepsilon_0 \psi_\sigma(t)\psi_u(t)\omega(r,\varphi,t,\varepsilon) = 0, \\ \tilde{\varphi}'(t) - \dfrac{v_0}{r} - \psi_v(t)\dfrac{\sigma_0}{r\psi_\sigma(t)} - \\ - \dfrac{2\varepsilon_0}{r}\psi_v(t)\omega(r,\varphi,t,\varepsilon) = 0, \\ \tilde{r}'(t) - \sigma_0 \psi_u(t)/\psi_\sigma(t) - 2\varepsilon_0 \psi_u(t)\omega(r,\varphi,t,\varepsilon) = 0. \end{cases} \tag{5}$$

$$\psi_u'(t) - \frac{2v_0\psi_v(t)}{r} - \frac{3}{2r}BD(\gamma_s - 1)\sigma_0^{\gamma_s - 2}\psi_\sigma(t) - $$
$$- \frac{\varepsilon_0 \psi^2{}_v(t)\omega(r,\varphi,t,\varepsilon)}{r} +$$
$$+ B\gamma_s(\gamma_s - 2)\psi_\sigma(t)\sigma_0^{\gamma_s - 3}\frac{\partial \sigma_0}{\partial r} = 0,$$

$$\begin{cases} \tilde{r}'(t) - B\gamma_s \sigma_0^{\gamma_s - 2}\psi_\sigma(t)/\psi_u(t) - \\ - B\gamma_s(\gamma_s - 2)\sigma_0^{\gamma_s - 3}\varepsilon_0 \psi_\sigma^2(t)/\psi_u(t)\omega(r,\varphi,t,\varepsilon) - \\ - \varepsilon_0 \psi_u(t)\omega(r,\varphi,t,\varepsilon) = 0, \\ \tilde{\varphi}'(t) - \dfrac{v_0}{r} - \dfrac{\psi_v(t)}{r}\varepsilon_0\omega(r,\varphi,t,\varepsilon) = 0. \end{cases} \tag{6}$$

$$\begin{cases} \psi_v'(t) + \psi_u(t)\dfrac{\partial v_0}{\partial r} + \dfrac{\psi_u(t)v_0}{r} + \dfrac{\psi_v(t)}{r}\dfrac{\partial v_0}{\partial \varphi} + \\ + \dfrac{\psi_u(t)\varepsilon_0\psi_v(t)\omega(r,\varphi,t,\varepsilon)}{r} + \\ + \dfrac{B\gamma_s}{r}(\gamma_s - 2)\psi_\sigma(t)\sigma_0^{\gamma_s - 3}\dfrac{\partial \sigma_0}{\partial \varphi} = 0, \\ \tilde{r}'(t) - \psi_u(t)\varepsilon_0\omega(r,\varphi,t,\varepsilon) = 0, \\ \tilde{\varphi}'(t) - \dfrac{v_0}{r} - \dfrac{B\gamma_s}{r}\sigma_0^{\gamma_s - 2}\psi_\sigma(t)/\psi_v(t) - \\ - \dfrac{B\gamma_s}{r}(\gamma_s - 2)\sigma_0^{\gamma_s - 3}\varepsilon_0\psi_\sigma^2(t)/\psi_v(t)\omega(r,\varphi,t,\varepsilon) - \\ - \dfrac{1}{r}\varepsilon_0\psi_v(t)\omega(r,\varphi,t,\varepsilon) = 0. \end{cases} \tag{7}$$

Let's analyze the equations containing $\tilde{r}'(t)$ . Then we receive conditions:

$$\psi_u(t)\varepsilon_0\omega(r,\varphi,t,\varepsilon) = B\gamma_s\sigma_0^{\gamma_s - 2}\psi_\sigma(t)/\psi_u(t) +$$
$$+ B\gamma_s(\gamma_s - 2)\sigma_0^{\gamma_s - 3}\varepsilon_0\psi_\sigma^2(t)/\psi_u(t)\omega(r,\varphi,t,\varepsilon) +$$
$$+ \varepsilon_0\psi_u(t)\omega(r,\varphi,t,\varepsilon) =$$
$$= \sigma_0\psi_u(t)/\psi_\sigma(t) + 2\varepsilon_0\psi_u(t)\omega(r,\varphi,t,\varepsilon)$$

From last equation we get:

$$B\gamma_s\sigma_0^{\gamma_s - 2}\psi_\sigma(t)/\psi_u(t) +$$
$$+ B\gamma_s(\gamma_s - 2)\sigma_0^{\gamma_s - 3}\varepsilon_0\psi_\sigma^2(t)/\psi_u(t)\omega(r,\varphi,t,\varepsilon) = 0, \tag{8}$$

$$\sigma_0 + (\gamma_s - 2)\varepsilon_0\psi_\sigma(t)\omega(r,\varphi,t,\varepsilon) = 0,$$
$$\sigma_0\psi_u(t)/\psi_\sigma(t) + \varepsilon_0\psi_u(t)\omega(r,\varphi,t,\varepsilon) = 0,$$
$$\sigma_0 + \varepsilon_0\psi_\sigma(t)\omega(r,\varphi,t,\varepsilon) = 0 . \tag{9}$$

Comparing (8) and (9) we see that $\gamma_s = 3$ . This result is very important because it corresponds to the case when the gas is in a state of ionized plasma. In addition, the ratio (9) shows that the surface density perturbation is negative.

Let us analize equations for $\tilde{\varphi}'(t)$ in systems (5)-(7). We get:

$$\psi_v(t)\frac{\sigma_0}{r\psi_\sigma(t)} + \frac{2\varepsilon_0}{r}\psi_v(t)\omega(r,\varphi,t,\varepsilon) =$$
$$= \frac{\psi_v(t)}{r}\varepsilon_0\omega(r,\varphi,t,\varepsilon).$$

From last equation we have:

$$\psi_v(t)\frac{\sigma_0}{r\psi_\sigma(t)} + \frac{\varepsilon_0}{r}\psi_v(t)\omega(r,\varphi,t,\varepsilon) = 0 .$$

We get equation (9).

Thus, we have system :

$$\begin{cases} \psi_\sigma'(t)+\sigma_0\dfrac{\psi_u(t)}{r}+\psi_u(t)\dfrac{\partial\sigma_0}{\partial r}+ \\ +\dfrac{\psi_v(t)}{r}\dfrac{\partial\sigma_0}{\partial\varphi}+\dfrac{1}{r}\varepsilon_0\psi_\sigma(t)\psi_u(t)\omega(r,\varphi,t,\varepsilon)=0, \\ \psi_u'(t)-\dfrac{2v_0\psi_v(t)}{r}-\dfrac{3}{r}BD\sigma_0\ \psi_\sigma(t)- \\ -\dfrac{\varepsilon_0{\psi^2}_v(t)\omega(r,\varphi,t,\varepsilon)}{r}+3B\psi_\sigma(t)\dfrac{\partial\sigma_0}{\partial r}=0, \\ \psi_v'(t)+\psi_u(t)\dfrac{\partial v_0}{\partial r}+\dfrac{\psi_v(t)}{r}\dfrac{\partial v_0}{\partial\varphi}+ \\ +\dfrac{\psi_u(t)v_0}{r}+\dfrac{\psi_u(t)\varepsilon_0\psi_v(t)\omega(r,\varphi,t,\varepsilon)}{r}=0, \\ \widetilde{\varphi}'(t)-\dfrac{v_0}{r}-\dfrac{\psi_v(t)}{r}\varepsilon_0\omega(r,\varphi,t,\varepsilon)=0, \\ \widetilde{r}'(t)-\psi_u(t)\varepsilon_0\omega(r,\varphi,t,\varepsilon)=0, \\ \sigma_0+\varepsilon_0\psi_\sigma(t)\omega(r,\varphi,t,\varepsilon)=0 \end{cases} \quad (10)$$

We will consider the system in t he area $G_\varepsilon^\alpha=\{(r,\varphi,t): g(r-\widetilde{r}(t))+g(\varphi-\widetilde{\varphi}(t))<\varepsilon^{1/\alpha_1}\}$. There are obvious inequalities in this area:

$$1\ge\omega(r,\varphi,t,\varepsilon)=1-\varepsilon^{1/\alpha_1-1}+O(\varepsilon^{2/\alpha_1-2}),$$
$$g(r-\widetilde{r}(t))<\varepsilon^{1/\alpha_1}.$$

Using this inequalities we get:

$$\left|r-\widetilde{r}(t)\right|<g^{-1}(\varepsilon^{1/\alpha_1})\ \text{ or }\ r=\widetilde{r}(t)+\alpha g^{-1}(\varepsilon^{1/\alpha_1}),$$
$$\alpha_1\in(-1,1).$$

Then

$$\frac{\partial\sigma_0(r)}{\partial r}=\frac{\partial\sigma_0(\widetilde{r}(t)+\alpha g^{-1}(\varepsilon^{1/\alpha_1}))}{\partial r}=$$
$$=\frac{\partial\sigma_0(\widetilde{r}(t))}{\partial r}+\alpha g^{-1}(\varepsilon^{1/\alpha_1})\frac{\partial^2\sigma_0(\widetilde{r}(t))}{\partial r^2}+$$
$$+o(\alpha g^{-1}(\varepsilon^{1/\alpha_1})).$$

Similarly, we can write other schedules. Then we get the following system, which will be executed with accuracy $O(g^{-1}(\varepsilon^{1/\alpha_1}))$ :

$$\psi_\sigma'(t)+\sigma_0\frac{\psi_u(t)}{\widetilde{r}(t)}+\psi_u(t)\frac{\partial\sigma_0}{\partial r}+\frac{\psi_v(t)}{\widetilde{r}(t)}\frac{\partial\sigma_0}{\partial\varphi}+$$
$$+\frac{1}{\widetilde{r}(t)}\varepsilon_0\psi_\sigma(t)\psi_u(t)=0,$$

$$\psi_u'(t)-\frac{2v_0\psi_v(t)}{\widetilde{r}(t)}-\frac{3}{\widetilde{r}(t)}BD\sigma_0\ \psi_\sigma(t)-$$
$$-\frac{\varepsilon_0{\psi^2}_v(t)}{\widetilde{r}(t)}+3B\psi_\sigma(t)\frac{\partial\sigma_0}{\partial r}=0,$$

$$\psi_v'(t)+\psi_u(t)\frac{\partial v_0}{\partial r}+\frac{\psi_v(t)}{\widetilde{r}(t)}\frac{\partial v_0}{\partial\varphi}+$$
$$+\frac{\psi_u(t)v_0}{\widetilde{r}(t)}+\frac{\psi_u(t)\varepsilon_0\psi_v(t)}{\widetilde{r}(t)}=0$$

$$\widetilde{\varphi}'(t)-\frac{v_0}{\widetilde{r}(t)}-\frac{\psi_v(t)}{\widetilde{r}(t)}\varepsilon_0=0,$$

$$\widetilde{r}'(t)-\psi_u(t)\varepsilon_0=0,$$

$$\sigma_0(\widetilde{r}(t),\widetilde{\varphi}(t),t)+\varepsilon_0\psi_\sigma(t)=0.$$

Taking into account last equations and condition *D=0* we get:

$$\begin{cases} \psi_u'(t)-\dfrac{2v_0\psi_v(t)}{\widetilde{r}(t)}-\dfrac{\varepsilon_0{\psi^2}_v(t)}{\widetilde{r}(t)}- \\ -3B\dfrac{\partial\sigma_0}{\partial r}\sigma_0(\widetilde{r}(t),\widetilde{\varphi}(t))/\varepsilon_0=0, \\ \psi_v'(t)+\psi_u(t)\dfrac{\partial v_0}{\partial r}+\dfrac{\psi_v(t)}{\widetilde{r}(t)}\dfrac{\partial v_0}{\partial\varphi}+ \\ +\dfrac{\psi_u(t)v_0}{\widetilde{r}(t)}+\dfrac{\psi_u(t)\varepsilon_0\psi_v(t)}{\widetilde{r}(t)}=0, \\ \widetilde{\varphi}'(t)-\dfrac{v_0}{\widetilde{r}(t)}-\dfrac{\psi_v(t)}{\widetilde{r}(t)}\varepsilon_0=0, \\ \widetilde{r}'(t)-\psi_u(t)\varepsilon_0=0, \end{cases} \quad (11)$$

$$\begin{cases} \dfrac{\partial\sigma_0}{\partial t}+\dfrac{v_0\partial\sigma_0}{r\partial\varphi}=0, \\ -\dfrac{{v_0}^2}{r}=-\dfrac{\partial\Phi_0}{\partial r}-B\gamma_s\sigma_0\ \dfrac{\partial\sigma_0}{\partial r}+\dfrac{3}{2r}DB{\sigma_0}^2, \\ \dfrac{\partial v_0}{\partial t}+\dfrac{v_0}{r}\dfrac{\partial v_0}{\partial\varphi}=-\sigma_0\ \dfrac{3B}{r}\dfrac{\partial\sigma_0}{\partial\varphi}. \end{cases} \quad (12)$$

## IV. Calculation of the trajectories of localized perturbations in the Mathcad environment

We will solve the system (11) in Mathcad 14.0 (see Fig.1.) In this case, we will simulate two solitons that have different velocities at the initial time. The initial conditions here are as follows. The first two values specify the radial and azimuthal components of the soliton velocity, the other two values are the initial coordinates of the soliton in the polar system, coordinate, radius and angle. We will consider the surface density as a function that depends only on the radius and choose it in the form:

$$g_0(r,\varphi)=C+Be^{-\alpha r}+\sum_{i=0}^{k}a_i e^{-\frac{(r-R_i)^2}{l_i}}. \quad (13)$$

The simulation result is shown on Fig.3. The two solitons (blue and red trajectories) start from the points (0,380), (0,390), the azimuthal components are the same, but the radial ones are different and equal to 5 and 54, respectively. Interestingly, the amplitude of oscillations does not change, as does the frequency. This can be seen in the graph of Fig.2.

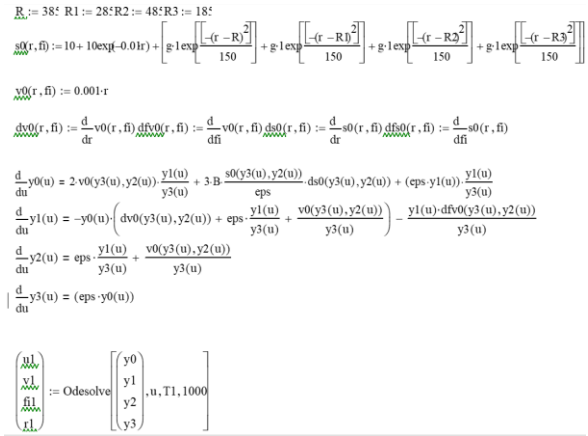

Figure 1. Example of Mathcad program for the system (11)

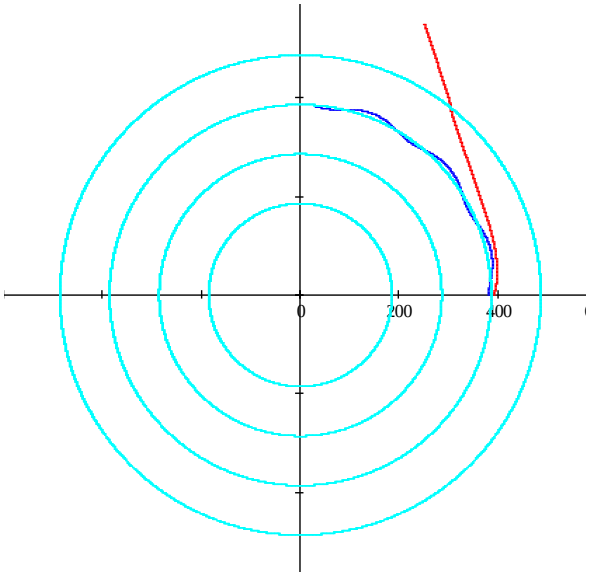


Figure 2. Trajectories of the two solitary waves

Initial condition for the waves are: first soliton (blue trajectiry on Fig.3): y0(0)=5, y1(0)=180, y2(0)=0, y3(0)=380, second soliton(red trajectory on Fig.3): y0(0)=58, y1(0)=180,y2(0)=0, y3(0)=390,T1=16.28, Eps=0.2, R=185, R1=285, R2=385, R3=485.

In this case, the second soliton (red), which had a higher initial velocity, moves along a curvilinear trajectory, approaching a circle where the density has a local maximum, intersects it, the trajectory is refracted like a ray of light and then becomes virtually rectilinear. We see that for a large T the soliton moves away from the center, asymptotically approaching the motion along some straight line, moving away from the center.

The corresponding behavior of a slower soliton can be interpreted in two ways: approximation to the region of maximum density and repulsion from the region of minimum. Note that we actually have an antisoliton here, a negative perturbation of density. Since the density changes continuously, the soliton is smoothly knocked out. If we had a clear boundary of the regions of density change, we would obviously have the phenomenon of embossing like Snelius's law. Thus, the soliton in a continuous medium will move in the direction of maximum density in areas where it is a smooth function and will be reflected in the presence of a sharp change in density.

Let us consider another example, when the density has circular areas with small values, the constants in (13) are: $C=11, B=0, k=4, l_i=15, R=385, R_1=285, R2=485, R_3=185, a_i=9.8.$

The graph of the function (13) is on Fig. 3. The initial conditions for the numerical experiment: first soliton (blue trajectiry on Fig.5): y0(0)=5, y1(0)=180,y2(0)=0, y3(0)=380, second soliton(red trajectory on Fig.4) : y0(0)=35, y1(0)=50,y2(0)=0, y3(0)=430.

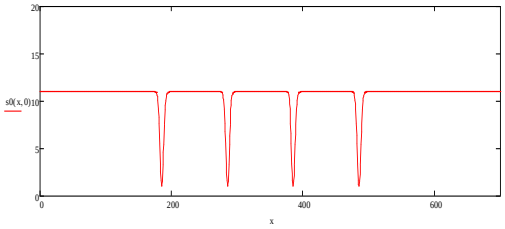


Figure 3. The graph of the surface density

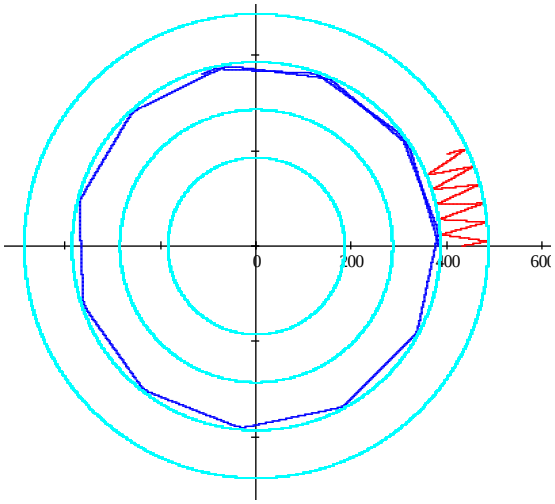


Figure 4. Example of the solitary wave trajectory

Other parameters are the same as in the previous example. On the Fig.5 we see that antisolitons at the corresponding initial velocities cannot penetrate regions with low density and are reflected in the same way as light quanta. The red antisoliton is reflected from both circular regions. This behavior of negative perturbations of the medium (localized regions of lower density) is in good agreement with the general properties of solitons, which are known to repel as elastic solids. Having a computer program, we can easily investigate the trajectories of solitary waves under any initial conditions.

## V. CONCLUSIONS

Thus, the paper considers the modeling of localized soliton-like perturbations in media whose characteristics are described by equations such as mile water. The specificity of the approach used here to study the trajectories of the corresponding perturbations is the assumption of the exact solutions of the corresponding

systems of equations and the use of the approximate approach.

As a result of using the method of T-representations, a system of differential equations is obtained, from which functions are obtained that describe the trajectories of localized waves. The system is solved using the Mathcad environment. It is shown that the corresponding software package is effective for cases when function compositions are used.

It is shown that the corresponding software package is effective for cases when function compositions are used. Solutions for different cases of surface density are found. It is shown that there are only antisolitons in the medium that are reflected from voids like light quanta, although the laws of reflection are essentially nonlinear. Theoretical analysis has shown that solitons occur in precipitation when the gas is in a state of ionized plasma. The obtained results correlate well with experimental studies, which confirms the adequacy of the applied approach to modeling and the possibility of using it for the development of wave monitoring software.

## REFERENCES


[1] V.I. Petviashvili, and O.A. Pokhotelov, "Solitary waves in plasmas and in the atmosphere," London: Routledge, 2016. doi:10.4324/9781315075556.

[2] S. Basak, R. Dutta, and P. S. Kar, "A new model with solitary waves: solution, stability and quasinormal modes," Eur. Phys. J. Plus, vol. 136, 2021, 618. Doi:10.1140/epjp/s13360-021-01544-3

[3] T. Asselmeyer-Maluga, and J. Kró, "Dark Matter as gravitational solitons in the weak field limit," Universe, vol. 6(12), 2020, 234. Doi: 10.3390/universe6120234

[4] L.A. Ureña-López, "Brief review on scalar field dark matter models," Front. Astron. Space Sci., vol. 6, 2019, pp. 1–13. Doi:10.3389/Fspas.2019.00047.

[5] E.W. Mielke, "Soliton model of dark matter and natural inflation," J. Phys. Conf. Ser., vol. 1208, 2019, 012012. Doi:10.1088/1742-6596/1208/1/012012.

[6] D. Bazeia, E. Belendryasova, and V.A. Gani, "Scattering of kinks of the sinh-deformed $\varphi^4$ model," Eur. Phys. J. C, vol. 78, 2018, 340. Doi: 10.1140/epjc/s10052-018-5815-z.

[7] A.R. Gomes, F.C. Simas, K.Z. Nobrega et al, "False vacuum decay in kink scattering," J. High Energ. Phys., vol. 2018, 2018, 192. Doi: 10.1007/JHEP10(2018)192

[8] D. Bazeia, A.R. Gomes, K.Z. Nobrega, and F.C. Simas, "Kink scattering in a hybrid model," Phys. Lett. B, vol. 793, 2019, pp. 26–32. Doi: 10.1016/j.physletb.2019.04.013

[9] P. Dorey, and T. Romanczukiewicz, "Resonant kink–antikink scattering through quasinormal modes," Phys. Lett. B, vol. 779, 2018, 117–123. Doi: 10.1016/j.physletb.2018.02.003

[10] P.D. Roy , J. Das, and S. Kar, "Quasi-normal modes in a symmetric triangular barrier," Eur. Phys. J. Plus, vol. 134, 2019, 571. Doi: 10.1140/epjp/i2019-12928-y

[11] P. D. Roy, S. Aneesh, and S. Kar, "Revisiting a family of wormholes: geometry, matter, scalar quasinormal modes and echoes," Eur. Phys. J. C, vol. 80, 2020, 850. Doi: 10.1140/epjc/s10052-020-8409-5

[12] Y.Turbal, M. Turbal, A. Bomba, and A. Sokh, "T-transformation method for studing the multi-solitone solutions of the Korteveg-de Vries type equations," Journal of Mathematics and System Sciense, vol. 4, 2015, 164–169. Doi: 10.17265/2159-5291/2015.07.001.

[13] N. Bila, E. Mansfield, and P.Clarkson, "Symmetry group analysis of the shallow water and semi–geostrophic equations," Q. J. Mech. Appl. Math, vol. 59, 2006, pp. 95–123.
A. Y. Bomba, and Y. V. Turbal, "Data Analysis Method and Problems of Identification of Trajectories of Solitary Waves," Journal of Automation and Information Sciences, vol. 47, 2015, pp. 13–23. Doi: 10.1615/JAutomatInfScien.v47.i10.20

[14] Y.Turbal, M. Turbal, A. Bomba, O. Radoveniuk "Method of Earthquake Prediction Based on the Soliton Mechanisms of Some Shocks," Journal of Environmental Science and Engineering, vol. 3 , 2014, pp. 151–155.